Lightning and Microphysical Characteristics of Incipient Local/Isolated Storms

Enrique V. Mattos[1,*], Luiz A. T. Machado[1], Earle R. Williams[2]

1. Instituto Nacional de Pesquisas Espaciais, Cachoeira Paulista, São Paulo, Brazil
2. Massachusetts Institute of Technology, Cambridge, Massachusetts, USA

ABSTRACT: The objective of this work was the evaluation of the electrical and microphysical characteristics of compact/isolated storms through the period from the first cloud-to-ground (CG) lightning flash. PPI images from X-Pol radar, and intracloud (IC) and cloud-to-ground strokes from BrasilDat and VHF sources from SPLMA during the CHUVA-Vale campaign have been used to characterize 74 incipient storms. The majority of first CG flashes are singles stroke with predominance of negative polarity. The compact negative center (~10 km of diameter) found in these storms, is a possible reason for the low multiplicity observed. However the interstroke time interval was similar (~72 ms) to that found in previous studies on multicellular storms with mesoscale organization. A dramatic decrease of Z_{dr} is observed after the first radar echo until the first CG flash, whereas the reflectivity increase quickly. That signature has been interpreted as the freezing of supercooled water in the mixed phase and the formation of graupel with conical form, whereas in the ice region, negative Z_{dr} is likely caused by vertically-aligned ice crystals in the cold phase (between -40° and -50°C).

INTRODUCTION

Incipient storms are an important target for cloud electricity studies. First, this select sub-group of storms provides a physical representation of the early development of storms. In that way, investigation of the lightning behavior in early stages enables the analysis of the most compact negative charge center possible. Additionally, from an operational view point, the compact and isolated nature of these storms provides an advantage in the use of radars operating at X-band (9.34 GHz), due the opportunity of avoiding severe attenuation and differential attenuation that can occur in developed mesoscale convection.

Several previous works have focused on the understanding of the stroke multiplicity and polarity in large cloud systems (like Squall Line and Mesoscale Convective System). The majority of previous work used a few cases studies, which can limit the physical interpretation. Also any consideration of the sequence of lightning (first, second or third flash) during the storm lifecycle has seldom been taken into account. Some questions still remain unanswered: What is the polarity and stroke multiplicity of first CG flash in compact/isolated storms? Is there a difference for those cases with mesoscale organization? For example, in Florida, Rakov and Uman (1990) found up to 17 strokes per flash, while in the New Mexico Kitagawa et al. (1962) found up to 26 strokes per flash in multi-cellular storms. The results from Saba et al. (2006) in São José dos Campos and Cachoeira Paulista in Brazil showed that 20 % of flashes analyzed

∗ Contact information: Enrique Vieira Mattos, INPE, Cachoeira Paulista, São Paulo, Brazil, Email: enrique.mattos@cptec.inpe.br

were single stroke and with a mean multiplicity of 3.8. The authors have emphasized the existence of a greater variability in these values from storm to storm. These previous results have shown the importance of verify a large dataset of storm and confirming if that variability is repeatable.

The hypotheses examined here is if in compact/isolated storms the negative charge center is small enough to preclude the existence of multiple strokes. In the microphysical view point, previous studies using polarimetric radar have shown that the occurrences of IC flashes are associated with graupel and hail in stronger updrafts. On the other hand, CG flashes have been observed close to the region of graupel and hail descending below the negative charge center (Goodman et al. 1989; López and Aubagnac 1997; Carey and Rutledge 1996; Tessendorf et al. 2007). However, an important question still remains unanswered: What is the typical behavior of supercooled water and ice particles from the first radar echo until the first CG flash in compact storms?

Recently, Ventura et al. (2013) reported a strong negative enhancement of the variable Z_{dr} (around -1.4 dB) before the maxima in -CG and +IC lightning rate, suggesting the vertical aligned of ice particles by strong electric field. Scattering simulations by Dolan and Rutledge (2009) have suggested the existence of vertically-aligned ice particles when Z_{dr} is between -2.1 and 0.5 dB in the temperature range -10° to -40°C and with lower reflectivity values (maximum of 32 dBZ). In contrast, graupel particles of high-density (0.5 g cm^{-3}) were characterized by a larger reflectivity (up to 54 dBZ), and smaller Z_{dr} values (-1.3 to 3.7 dB). Another hypothesis for negative Z_{dr} before lightning occurrence is the existence of gravity-aligned graupel with conical form. For example, Evaristo et al. (2013) showed that the Z_{dr} from conical graupel decreased linearly when the cone apex angle decreased. A Z_{dr} value of -1.2 dB was obtained for 30° and +0.8 dB for a 70° apex angle. However, that hypothesis has not been tested directly in the presence of lightning. There is a shortcoming in the literature, on the discussion of these signatures in mixed phase of conical graupel aligned by the gravitational field and ice crystals vertically aligned by a strong electric field. We have addressed that question in this study, combining an X-band radar and a VHF and VLF lightning network.

To answer the principal question addressed above, we identified and tracked 74 incipient storms using the X-band radar during November, 2012 and March, 2012 in São José dos Campos, Brazil. Lightning data from BrasilDat were used to determine stroke multiplicity and polarity of the first IC and CG flash. The SPLMA was utilized to characterize the electrical structure and initiation region for two storms.

DATA AND METHODOLOGY

An X-band polarimetric (X-Pol) radar operated during the CHUVA-Vale campaign between November 2011 and March 2012 in São José dos Campos was utilized to identify and track incipient storms. The radar executed a volumetric scan every 4 min with maximum range of 100 km and radial resolution of 150 m. Plan Position Indicator (PPI) images from 13 elevations were utilized and the principal variables used were: horizontal reflectivity (Z_h, dBZ), differential reflectivity (Z_{dr}, dB) and specific differential phase (K_{dp}, °km^{-1}). The attenuation correction and determination of the Z_{dr} offset were performed before the utilization of radar data. Also the wet radome correction was applied with rainrate measured by a raingauge close to the radar. Two lightning networks (VLF and VHF) have been utilized to analyze the physical characteristics of first lightning flashes during the CHUVA-Vale campaign. The first dataset is related to time, peak current and polarity of strokes from BrasilDat. For studies of the electrical structure of storms VHF sources from SPLMA have been used. The SPLMA was composed of 12 sensors installed 15-30 km apart with a network diameter of approximately 60 km. (Bailey et al. 2011). Fig. 1 shows the locations of the X-Pol radar (gray triangle), BrasilDat (blue stars) and SPLMA (red circles) sensors.

The first step was the grouping of intracloud and cloud-to-ground strokes in each lightning flash. A time and space window of 0.5 sec and 20 km were used, respectively. Each storm was defined using the azimuth angle and the radar range to delimit the boundary of storms. For each storm the number of flashes (intracloud and cloud-to-ground) and VHF sources were counted during 6 min time intervals. The maximum reflectivity for every elevation (13 PPI's) was searched and the coincident Z_{dr} and K_{dp} values were extracted from those locations. The size of the storm is determined by considering the reflectivity area in the PPI scan (closest to 6 km altitude) exceeding 20 dBZ at the time of the first cloud-to-ground flash. That region is an approximation for the negative charge center (close to -10°C) in typical storms. The data analysis is continued through histograms of stroke multiplicity, size, and interstroke intervals. The behavior of the vertical profile of Z_h, Z_{dr}, and K_{dp} from the first radar echo until the first cloud-to-ground flash was studied.

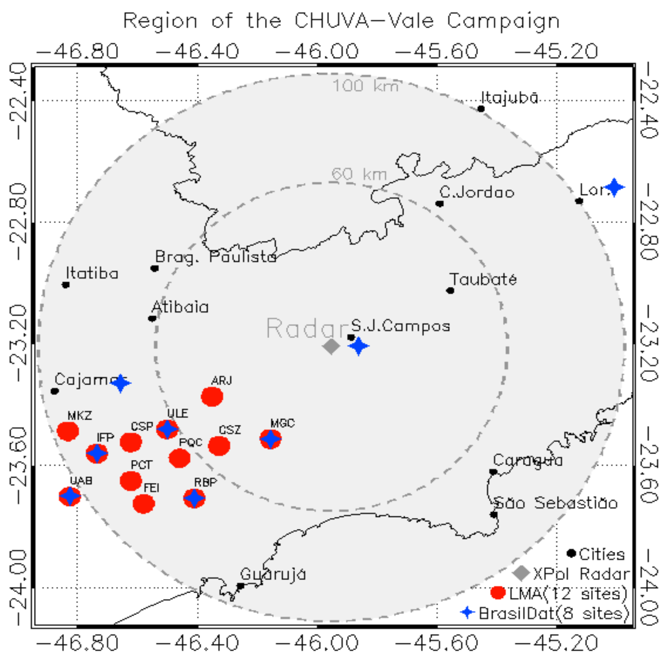

Figure 1 – Map showing the region of the CHUVA-Vale campaign. The locations of the X-Pol radar (gray triangle), the positions of the BrasilDat (blue stars) and SPLMA network sensors (red circles), and principal nearby cities (black dots) are shown.

RESULTS AND DISCUSSION

The size distribution of storms is shown in Fig. 2. The size was determined by considering the area within the 20 dBZ reflectivity threshold and equating that area to a circular area of radius R. The majority of storms had size between 3 and 6 km radius, with some cases reaching 8 km. The mean size determined was 5 km, which implied a 10 km diameter. That estimate supports the notion of compact storms. Assuming that the majority of negative space charge is carried by radar-detected precipitation, this size calculation provided an estimative of the negative charge area.

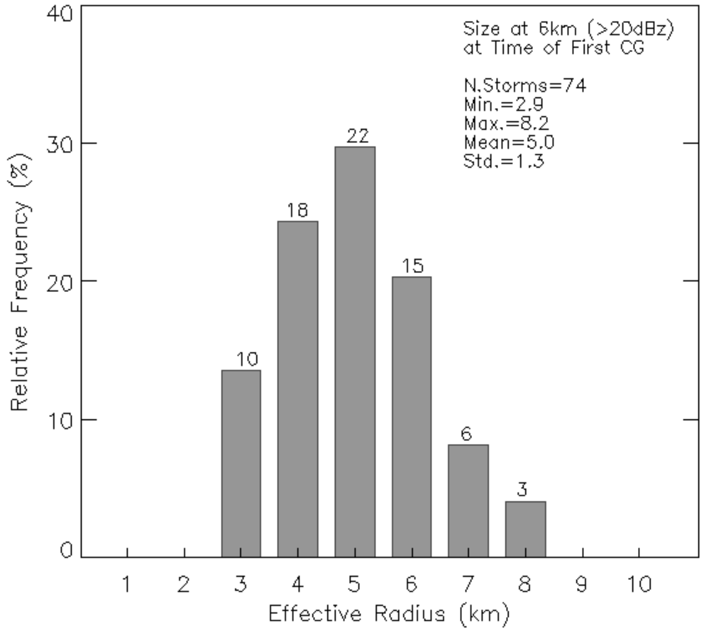

Figure 2 – Distribution of measured effective radii (km) for the 74 incipients storms. That size is estimated considering a circular area of radius R equal to the total radar-measured area of reflectivity > 20 dBZ, at an altitude of 6 km. The storms studied are very compact. The largest storm shows a 16 km diameter.

Fig. 3 shows the distribution of stroke multiplicity for (a) intracloud and (b) cloud-to-ground flashes. Whereas the physical characteristics of CG flashes are well reported and discussed in the literature, IC flashes have few observations. For the first (Fig. 3b), no multiplicity greater than two was observed for CG flashes. 75 % of cases showed singles strokes. That result differs markedly with previous studies (Rakov and Uman 1990; Kitagawa et al. 1962). Basically these earlier studies found flashes with higher multiplicity, sometimes reaching 26 strokes per flash. The majority of previous studies have considered large storm systems: Squall Lines and Mesoscale Convective Systems. That suggests that the size of the negative charge center is a key feature for determining the number of strokes possible in one flash. Also the absence of additional charge in compact storms appears to suppress flashes with multiples strokes. The IC flashes showed higher multiplicity. The maximum number of strokes per flash was four, but the majority (60%) of cases showed single strokes (Fig. 3a). The multiplicity metric in intracloud flashes is not completely understood. Usually a better terminology will be “intracloud pulse” instead of “intracloud multiplicity”.

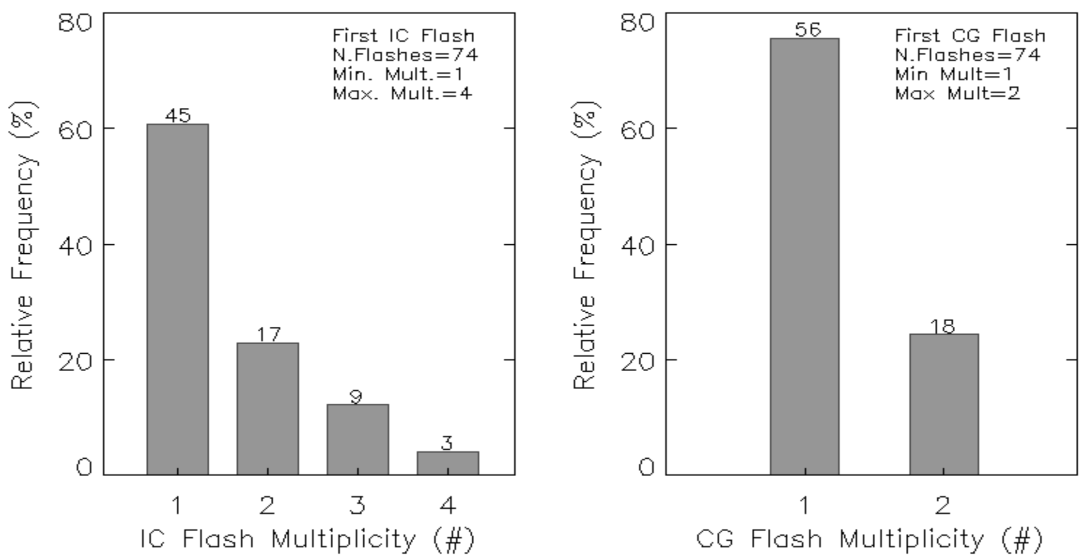

Figure 3 - Distribution of stroke multiplicity for (a) intracloud and (b) cloud-to-ground flashes from 74 incipient storms. The majority of first CG flashes show single stroke behavior.

An important physical characteristic of the flashes with multiples strokes is the interstroke time interval. The distribution of interstroke time intervals is presented in Fig. 4. For CG flashes (Fig. 4b) the mean time interval observed was 72 ms. The highest frequency of occurrence for these cases was 50-70 ms. That time interval is comparable with previous studies in larger, multi-cellular storms. For example, Saba et al. (2006) found a mean interstroke interval of 61 ms for flashes that followed the same channel to ground and also for flashes that that followed a different channel. Considering a typical horizontal velocity of 5×10^4 ms^{-1} for the positive leader inside the negative center, a horizontal distance of 3.6 km is determined. That distance is an appreciable part of the size of the storms documented here (~ 10 km of diameter, Fig. 2). For the majority of IC flashes, a time interval around 10 ms was observed, which is much smaller than the valued found for CG flashes (72 ms). The closer proximity of the charge center inside the cloud than the distance between the cloud and the ground can be responsible for this shorter time. There is no clear difference in the time interval between IC flashes with two, three and four strokes per flash. However, only the flash with higher multiplicity (four strokes by flash) showed the largest time interval (~250 ms). That suggests a dependence of time interval on the total duration of flash.

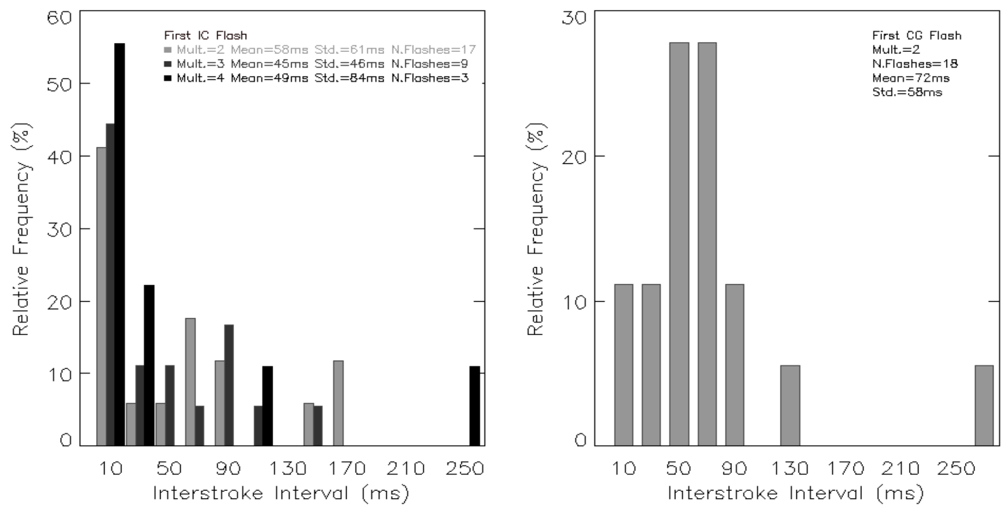

Figure 4 - Distribution of interstroke time intervals (ms) for (a) intracloud and (b) cloud-to-ground flashes for 74 incipient storms. The intracloud flashes are shown by multiplicity: two (light gray box), three (dark gray box) and four strokes (black box). The mean CG flash interstroke interval is 72 ms, which is similar to that found in previous studies from multicellular storms.

Another focus of this work is the characterization of the behavior of supercooled water and ice particles before the first CG flash. The temporal evolution of a storm case (case#003) from the first radar echo until the first CG flash is shown in Fig. 5. The storm started with a reflectivity around 20 dBZ (Fig. 5a), whereas the differential reflectivity was around +2 dB (Fig. 5b). Supercooled raindrops are evident in that moment above the melting layer. After that time a quick freeze (negative Z_{dr} ~-1dB) and formation of larger ice crystal occurs until before the first CG flash. The higher reflectivity (50 dBZ) and negative Z_{dr} (-1dB) between 4.4 and 9 km (0° and -40°C) suggested a signature from graupel with conical form. Noteworthy is the observation that after the first CG the minimum Z_{dr} shows a flat behavior, with a constant value around -0.5 dB. That observation can be indicating that the concentration and orientation of the hydrometers has not changed much after the first flash, due the small area associated with these incipients storms. Also a better temporal resolution or a measurement with fixed pointing of the radar beam will likely better describe the rapid changes and re-orientation of ice crystals by the electric field change in lightning flashes. For the majority of cases analyzed (74 in the total) the flat behavior of Z_{dr} is repeatable.

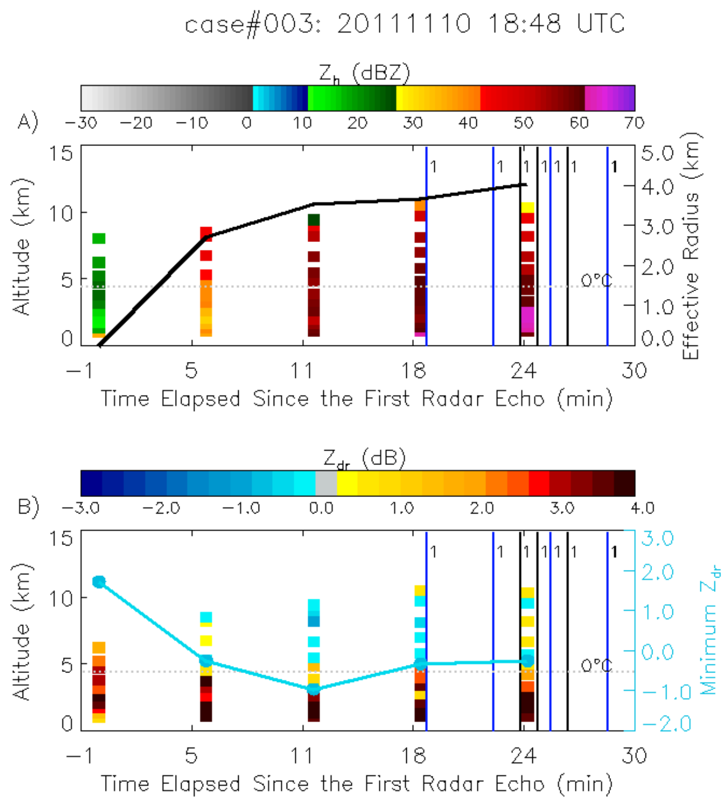

Figure 5 - Time-height plot of storm evolution (case#003) on November 10, 2011 beginning at 18:48 UTC. (a) reflectivity in horizontal polarization (Z_h, dBZ) and (b) differential reflectivity (Z_{dr}, dB). The black line in (a) is the effective radius at 6 km altitude for the region with more than 20 dBZ and the blue line in (b) is the minimum Z_{dr} value in the profile. The blue and black vertical lines in both figures denote the times of the CG and IC flashes, and the numbers to the right of each vertical line are the multiplicities of that flash.

CONCLUSIONS

For the first time the microphysical and electrical characteristics of a large (> 70) dataset of incipient storms has been analyzed. Due to the compact nature of the negative charge center (~10 km), the majority of first cloud-to-ground flashes are single stroke and with negative polarity. The initiation of precipitation in those storms is associated with the formation of supercooled raindrops, as shown by stronger positive Z_{dr} above 0°C. The appearance vertically-aligned ice particles in the cold phase and some signature from conical graupel in mixed phase becomes clear.

ACKNOWLEDGMENTS

We would like to thank the CHUVA project (grant 2009/15235-8). The first author was financed with a graduate fellowship from FAPESP (2013/04292-6). The third author has participated of CHUVA-Vale campaign trough FAPESP project grant 2011/13673-8. We would like to thank the GOES-R program, which made the LMA network available in the CHUVA project. Thanks to J. Bailey and R. Blakeslee for providing and reprocessing the LMA data and for all discussions on the network. We also thank K. Naccarato and S. Heckman for discussions on the BrasilDat network and its data.

REFERENCES

Bailey, J. C., L. D. Carey, R. J. Blakeslee, S. J. Goodman, R. Albrecht, C. A. Morales, and O. Pinto Jr.,: São Paulo Lightning Mapping Array (SP-LMA): Deployment and plans. Proceedings, *XIV International Conference on Atmospheric Electricity*, Rio de Janeiro, RJ, ICAE, 1-4, 2011.

Carey, L. D., and S. A. Rutledge, 1996: A multiparameter radar case study of the microphysical and kinematic evolution of a lightning producing storm. *Meteorol. Atmos. Phys.*, **59**, 33-64.

Dolan, B., and S. A. Rutledge, 2009: A theory-based hydrometeor identification algorithm for X-band polarimetric radars. *J. Atmos. Oceanic Technol.*, **26**, 2071-2088.

Evaristo, R., T. M. Bals-Elsholz, E. R. Williams, D. J. Smalley, M. F. Donovan, and A. Fenn, 2013: Relationship of graupel shape to differential reflectivity: Theory and observations. Proceedings, *93rd Amer. Meteor. Soc. Annual Meeting*, Austin, TX, Amer. Meteor. Soc., 1-9.

Goodman, S. J., D. E. Buechler, P. D. Wright, W. D. Rust, and K. E. Nielsen, 1989: Polarization radar and electrical observations of microburst producing storms during COHMEX. Proceedings, *24th Conference on Radar Meteorology*, Tallahassee, FL, Am. Meteorol. Soc., 109-112.

Kitagawa, N., M. Brook, and E. J. Workman, 1962: Continuing currents in cloud-to-ground lightning discharges. *J. Geophys. Res.*, **67**, 637-647.

López, R. E., and J-P. Aubagnac, 1997: The lightning activity of a hailstorm as a function of changes in its microphysical characteristics inferred from polarimetric radar observations. *J. Geophys. Res.*, **102**, 16799-16813.

Rakov, V. A. and M. A. Uman, 1990: Some properties of negative cloud-to-ground lightning flashes versus stroke order. *J. Geophys. Res.*, **95**, 5447-5453.

Saba, M. M. F., M. G. Ballarotti and O. Pinto, Jr., 2006: Negative cloud-to-ground lightning properties from high-speed video observations. *J. Geophys. Res*., **111**, D3.

Tessendorf, S. A., S. A. Rutledge, and K. C. Wiens, 2007: Radar and lightning observations of normal and inverted polarity multicellular storms from STEPS. *Mon. Weather Rev.*, **135**, 3682-3706.

Ventura, J. F., F. Honoré, and P. Tabary, 2013: X-band polarimetric weather radar observations of a hailstorm. *J. Atmos. Oceanic Technol.*, **30**, 2143-2151.